Modelling of low energy/low velocity impact on Nomex honeycomb sandwich structures with metallic skins

Bruno Castanié, Christophe Bouvet, Y. Aminanda, J.-J. J.-J. Barrau, P. Thevenet

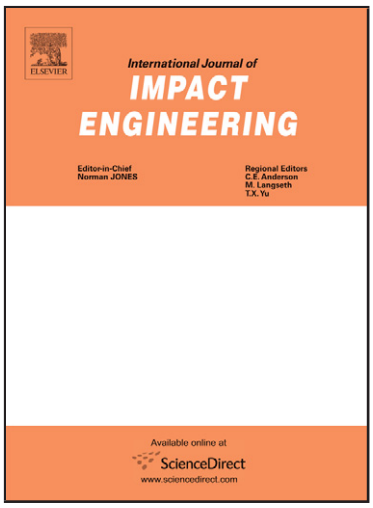

www.elsevier.com/locate/ijimpeng

Modelling of low energy/low velocity impact on Nomex honeycomb sandwich structures with metallic skins

B. Castanié, C. Bouvet, Y. Aminanda, J.-J. Barrau, P. Thevenet

PII: S0734-743X(07)00028-0
DOI: doi:10.1016/j.ijimpeng.2007.02.008
Reference: IE 1466

To appear in: *International Journal of Impact*

Received date: 25 September 2006
Revised date: 8 November 2006
Accepted date: 28 February 2007

Cite this article as: B. Castanié, C. Bouvet, Y. Aminanda, J.-J. Barrau and P. Thevenet, Modelling of low energy/low velocity impact on Nomex honeycomb sandwich structures with metallic skins, *International Journal of Impact* (2007), doi:10.1016/j.ijimpeng.2007.02.008

MODELLING OF LOW ENERGY/LOW VELOCITY IMPACT ON NOMEX HONEYCOMB SANDWICH STRUCTURES WITH METALLIC SKINS.

B. Castanié*, C. Bouvet*, Y. Aminanda**, **J-J. Barrau *****, **P. Thevenet†**

**IGMT, LMS Supaéro, BP 4032, 31055 Toulouse Cedex 4, France*
***Mechanical Engineering Dept of IIUM, Jl. Gombak P.O. Box 10 50728 Kuala Lumpur, Malaysia.*
**** LGMT, Bat 3PN, Université Paul Sabatier, 118 Rte de Narbonne, 31062 Toulouse, France*
† *EADS CCR, 12 rue Pasteur, BP 76, 92152 Suresnes Cedex, France*

Corresponding author: bcastani@cict.fr, Tel: 33.(0) 5.62.17.81.16. Fax: 33.(0)5.61.55.81.78.

Abstract.

In the aircraft industry, manufacturers have to decide quickly whether an impacted sandwich needs repairing or not. Certain computation tools exist at present but they are very time consuming and they also fail to perfectly model the physical phenomena involved in an impact. In a previous publication, the authors demonstrated the possibility of representing the Nomex™ honeycomb core by a grid of nonlinear springs and have pointed out both the structural behaviour of the honeycomb and the influence of core-skin boundary conditions. This discrete approach accurately predicts the static indentation on honeycomb core alone and the indentation on sandwich structure with metal skins supported on rigid flat support. In this study, the domain of validity of this approach is investigated. It is found that the approach is not valid for sharp projectiles on thin skins. In any case, the spring elements used to model the honeycomb cannot take into account the transverse shear that occurs in the core during the bending of a sandwich. To overcome this strong limitation, a multi-level approach is proposed in the present article. In this approach, the sandwich structure is modelled by Mindlin plate elements and the computed static contact law is implemented in a non linear spring located between the impactor and the structure. Thus, it is possible to predict the dynamic structural

response in the case of low-velocity/low-energy impact on metal-skinned sandwich structures. A good correlation with dynamic experimental tests is achieved.

Keywords.

Sandwich structures, low velocity/low energy impact, finite element nonlinear analysis, indentation.

1-Introduction

Sandwich structures exhibit static properties such as high stiffness-to-weight ratio and high buckling loads which are of great importance in the aeronautics field. Nevertheless, the current applications on commercial airplanes remain mainly limited to secondary structures like control surface or floor panels. In the field of helicopters where stress levels are lower, full sandwich structures are already in flight. In fact, one of the main limitations is linked to a lack of knowledge on the effects induced by impact damages [1]. However, in service, such structures are exposed and are often impacted during taxiing manoeuvres or take-off. They can also be damaged by tool drops during maintenance operations [2] and [3]. In such circumstances, the aircraft manufacturer has to inform the users very quickly of whether the impacted structure needs a repair or not. The study presented in this article is a step toward the final objective, which is to provide the aerospace industry with an inverse method. In this method, a 3D picture of the damage is first made by the airline company. Then, based on the shape of the impact, the impactor's shape is found and both the impact damage and the residual strength would be computed.

This article investigates low speed and low energy impact phenomena. Tests in industry and most publications agree that, in this type of impact and for aeronautical sandwiches with

skins that not exceed 2.5 mm, there is an equivalence between dynamic tests and static indentations [4], [5] and [6]. However, static tests have the advantage of being easier to set up and show low dispersion. This hypothesis will also be assumed in this study. At this first stage, the study will focus on modelling impacts on sandwich structures with Nomex™ honeycomb core and metallic skins. Metallic skins are used in order to avoid the complex mechanisms of laminate skins damaging.

The indentation response of sandwich structures can be determined by using Meyer's law with experimentally correlated coefficients, spring-mass models or energy-balance models [1]. Analytical models of beams or plates on elastic foundations have also been developed by several authors [7]. The first approaches were based on elasticity theory, so their practical use remains limited [1]. Soden [8] and Olsson [9] used a foundation model with a perfect plastic law which may be able to represent the core behaviour. The model of Soden is also geometrically nonlinear. However, because the core crushes [10] and [11] and the skin plasticizes, this type of approach also remains limited. The damage of the core also proves to be very important as it even occurs at the weakest energies and without any visible damage on laminated skins.

Certainly, understanding and modelling the crushing phenomenon are the key points of the general problem of impact on sandwich structures with honeycomb. Core crushing is a complex mechanical phenomenon characterized by the appearance of various folds and failures in the hexagonal structure. This phenomenon is known for its energy-absorbing capacities and has been analysed since 1963 by Mc Farland [12]. The crushing of aluminium honeycomb core has been extensively studied by Wierzbicki et Al [13] [14] and, more recently, by Mohr et Al [15]-[17]. Constitutive equivalent models have been developed [18], [19] and have been applied successfully to experiments on large structures subjected to blast

loads. However, complex multiaxial experiments on honeycomb are required to identify the crushing laws and, as pointed out by Vaziri [20], the models are not suitable for simulating the phenomenon locally. Besides, the developments apply to metallic honeycomb only. It appears that Nomex™ honeycomb has a more complex micromechanical behaviour. Matrix cracking at the surface and local detachment and tears are observed [11] and [21]. Conventionally, modelling of this phenomenon is either based on an equivalent material law, which could be of the perfectly plastic type [22] and [23], or on a discrete crushing law (with a peak) for honeycomb blocks [24] and [25]. In this area, Horrigan [26] used an isotropic continuum damage model, but this modelling was limited to small indentations, since the continuity of the damage model and the plastic stress flow did not represent the real damage in the core.

All the approaches presented have a common feature which is to consider the honeycomb as a homogeneous material. Recently, based on a phenomenological approach and a structural analysis of honeycomb core with "soft" materials like paper or Nomex™, the authors have proposed a discrete modelling of the honeycomb [27]. A crushing law, including the influence of the boundary conditions which take into account the interaction between the skin and the honeycomb, was proposed. It predicts the static indentation of metal-skinned sandwiches supported on rigid flat support [28]. Those two points will be recalled in the first part of this article and an investigation of the domain of validity of this approach will be developed. It is noticeable that this approach can also predict the residual dent and the extension of the damage during compression after impact testing [29]. An original criterion of structural strength in compression after impact (CAI) based on the collapse of cells at the edge of the impacted area was also proposed. The main limitation of this model is the fact that the vertical grid of nonlinear springs modelling the honeycomb core obviously cannot take

into account the transverse shear stress. This limitation will be solved by demonstrating that the local indentation and the flexural response can be superimposed in static tests on a simply-supported sandwich structure. Then the method will be extended to dynamic tests that finally provide a multi-level approach.

2- Justification and limitation of the discrete modelling of honeycomb core

In this part, the key points of the work presented in Aminanda [27], [28] are first summarized. Several uniform compression tests were conducted on honeycomb block with three different materials (paper, Nomex™ and aluminium). Each block of honeycomb was also bonded to one or two skins to simulate two types of boundary conditions between the honeycomb and the compression plate. Large cells were made for the paper honeycomb which allowed the mechanism of deformation to be observed easily. For a specimen with one skin, local buckling on one side of the free surfaces of the honeycomb occurred for very low loads while the vertical edge of the cell remained straight (Figure n°1). In the case of Nomex™ honeycomb, because of the small dimensions of the cells, it was not so easy to observe the mechanism. Nevertheless, a finite elements model showed that this local buckling occur at 20 % to 50 % of the peak or maximum load. The phenomenon seems to be triggered by the simply-supported boundary conditions on this free surface which allow local rotation of the cell walls. This sensitivity is also found on the force-displacement curves (Figure n°2). For two-skin Nomex and Paper specimens the peak force was pronounced and the difference with the maximum force of one-skin specimens was significant. However, the difference was smaller for aluminium honeycomb, a reduction of about 10 % being observed. The Young modulus of aluminium is thirty times that of Nomex and the greater stiffness of the wall can

partially explain the reduction. Therefore, it seems that the sensitivity to boundary conditions must be taken into account only in the case of "soft materials".

Since local buckling occurs early, the honeycomb structure works in a postbuckling mode and an analogy can be made with stiffened structures under compression in aircraft (Figure n°3). The stiffener in honeycomb is the vertical edge that is formed by the intersection of 3 cell wall. When the skin buckles, the compressive stress in the skin cannot be more than the buckling stress and the compression excess is therefore taken up by the stiffener and the nearby skin, with an equivalent half width equal to fifteen times the skin thickness (15.e) [30]-[31]. By analogy, for the honeycomb cell, the compression is mainly taken by the vertical edges since the buckling of the walls occurs earlier. Then the collapse of the stiffened structure corresponds to the buckling of the stiffeners. In the case of honeycomb there is no collapse but, rather folding. The previous analysis shows that only the cell edge plays an important role from a structural point of view. This reasoning leads to the hypothesis that Nomex™ honeycombs under a crushing force behave like a juxtaposition of vertical cell edges and it is possible to model them by a grid of vertical nonlinear springs located at the angles of the hexagons (see Figure n°4). Furthermore, the local rotations must be taken into account as they modify the crush law of cell edge from a "with-peak" law to a "no peak" law. So, the following form is proposed for a generalized crush law of a cell edge:

$$F_i = F_{Crush}(w_i, \theta_i) + \sum_{j=1}^{3} F_{shear} \cdot H(w_i - w_j - w_{Limit}) \qquad \text{(eq 1)}$$

Where w_i and θ_i are the vertical depth of crush and the local rotation on the upper part of cell edge i. w_j , j = 1 to 3 are the crushing depth of the adjacent edges.

The function $F_{Crush}(w_i , \theta_i)$ is plotted in Figure n°5. The following variation is proposed:

- if $\theta_i = 0$ the experimental "with peak" F_{wp} law is used (see the "two-skins" curve).

- if $\theta_i >= \theta_{critical}$ then a "no peak" law F_{np} is used.
- if $0 < \theta_i < \theta_{critical}$ then an intermediate law F_i is defined.

The crush law for one edge "with peak", F_{wp} is obtained by dividing the experimental compression law by the number of edges. The law presented was obtained using experiments on a Nomex™ honeycomb block (HRH78, 1/8-3 of 48kg/m^3 and 15 mm thick) containing 100 cells (10 on each side). The specimens were prepared by carefully cutting the specimen to preserve the vertical edges on the outer side of the honeycomb block (inset in Figure n°2). The total number of cell edges of this block was 240.

The threshold parameter $\theta_{critical}$ was identified by performing indentation tests on sandwich structures [28]. For the range of sandwich structures used in the experiments, this value was about 2.3°. $H(w_i - w_j - w_{limit})$ is a Heaviside function with:

$$H(w_i - w_j - w_{Limit}) = 0 \text{ if } w_i - w_j - w_{Limit} \leq 0$$
$$H(w_i - w_j - w_{Limit}) = 1 \text{ if } w_i - w_j - w_{Limit} > 0$$

The influence of F_{shear} was investigated and w_{Limit} was determined by means of tests using cylindrical indenters which created shear stress in the walls located in the circumferential zone of the indenter as explained by Wierzbicki et al [14]. Quasi-static tests using 3 different radii (8, 14.75 and 25 mm) of cylindrical indenters were conducted on the same honeycomb (see Figure n°6). Two tests were performed for each radius but only single-test curves are presented because the behaviour is hardly varied. The circumference of the cylindrical indenter can be observed to coincide either with a vertical edge (POINT 1, Figure n°6) or with a wall (POINT 2, Figure n°6). According to the position on the circumference, it can be assumed that either the edge is subjected to compression or the wall is under shear load.

Figure n°7 compares the contact laws obtained from experiment and computation on discrete model not taking into account the shear of the walls, for the three indenters, in terms

of force versus indentation depth. The curves are nearly superimposed at the beginning and the difference starts to appear from a point corresponding to the shear of the wall in the circumferential zone. It is interesting to note that this difference begins to appear at indentation depths of about 0.32 mm independently of the indenter diameter. It should also be noted that the number of cell walls on the circumferential zone is proportional to the radius of the indenter. There were 18, 30 and 56 cells for radii of 8, 14.75 and 25 mm respectively. Since it is assumed that these walls are subjected to shear load, in consequence the shear force is also proportional to the indenter radius. This additional shear force, F_{Sup} can be expressed as:

$$F_{Sup} = 2\pi.r.q_{shear}$$

where r is the radius of the cylindrical indenter and q_{shear} is the shear force per unit length in the circumferential zone. The unit shear force q_{shear} can thus be obtained by dividing the difference between the computation and the test by $2\pi.r$. Calculations show that the unit force q_{shear} is not very different for the three indenter radii (Figure n°8). However, the peak force is lower for the 8 mm radius possibly because of the greater dispersion due to the location of the indenter and the small number of walls sheared. This result globally confirms the hypothesis that the extra indentation force is taken up by peripheral shearing and is in agreement with Wierzbicki's results [14].

The results also demonstrate that the additional force, due to shear only, occurs from a certain indentation depth limit: Δw_{Limit} =0.32 mm. *Below this threshold, the error induced by assuming that the honeycomb can be modelled simply by its vertical edges, which behave independently of each other and are subjected only to compression load, seems to be negligible.* A simple geometrical analysis (Figure n°9) shows that the corresponding limit angle is 0.27 rad, about 15°. This calculation was performed assuming

that the circumference of the indenter passed through the middle of the cell, which avoided having to take the reaction of the vertical edge into account. It was then verified a posteriori that, in the case of the indentation experiments using spherical indenters [27], this limit was not reached. The limit angle varied between 0.007 rad (radius 57.25mm) and 0.025 rad (radius 16.25mm) which is well below the calculated threshold. To see if the angle obtained had a real physical meaning, a complementary test was carried out with a conical indenter of half-angle 18° (> 15°) at the summit. It was observed that the edge-independence hypothesis still remained valid as the correlation between calculation and test results was very good (Figure n°10), which suggests that the actual threshold is little higher.

In consequence, for the indentation of a sandwich structure, it will be possible to model the honeycomb by its vertical edges alone if the deformation of the skin is not too pronounced and the difference in crushing between two neighbouring edges does not exceed w_{Limit}, which is generally the case. For all our studies, w_i-w_j was always less than w_{limit}. Therefore, we did not try to determine the F_{shear} law because it is only needed for sharp projectiles on thin skins. In such cases, the skin is generally perforated which is out of the scope of our research.

3-Computation of the static contact law

Experiments and numerical studies were carried out on sandwich structures with metal skin and the same Nomex™ honeycomb core as described in the last paragraph. Metal skins were used in order to avoid the complex failure damage mode of composite laminated skin.

3.1 Experimental investigations

Quasi-static indentation test were carried out on 100 x 100 mm sandwich structures. Brass skins of 0.1 and 1 mm thickness were bonded to the Nomex™ honeycomb with a layer

of REDUX™ 312/5 glue. Tension tests were performed on brass skin specimens for the two different thicknesses. For the 0.1 mm specimen, the elastic modulus was 103100 MPa and the yield stress was about 433 MPa. For the 1 mm specimen the elastic modulus was 70400 MPa and the yield stress was about 104 MPa. Obviously, alloys differ. Then, several specimens were made, as listed in . Indentation of all specimens was done using the same INSTRON™ machine and the same spherical indenters having different radii (57.25, 30.125 and 21.75 mm). Tests were performed with speed of 0.5 mm/minute, which can be considered as quasi-static loading. The specimens were fully supported on a rigid metallic part (Figure n°11). The loads were measured by the machine's sensor but displacements were measured using a dial comparator positioned on the indenter. Three tests were completed for each type of sandwich structure (with thin or thick skin) and for each indenter. The experimental contact laws are partially presented in Figure n°12, (0.1 mm skin) and (1 mm skin). The contact laws obtained show a low dispersion on the results in the case of 0.1 mm skins. This dispersion is higher for the 1 mm skin specimen (about 10%). For the 0.1 mm thin skin, the aspect of the crush curves shows nothing out of the ordinary, with the exception of small undulations which are similar to those observed on indentation on honeycomb alone. For the 1 mm thick skin, the curve shows a very high stiffness at the beginning of the indentation (because the bending stiffness was 1000 times that of the 0.1 mm specimens) which becomes weaker afterwards. This change can be qualitatively attributed to the collapse of the first honeycomb cell under the indenter. Indeed, the change of curve slope is observed for a penetration value (0.29 mm) which corresponds to the results obtained previously on the uniform compression test on the honeycomb alone. At that time, a noise corresponding to the breaking of the honeycomb was heard.

3.2 Comparison between computation and experiment.

An implicit nonlinear finite element model was made (see Figure n°14). The software used was the SAMCEF™ code *(by SAMTECH GROUP)*. Nonlinear springs were placed at the same location as the honeycomb cell angles. The generalized law was implemented using special features of the software. The metal skins were modelled by Mindlin plate elements for thin skin (0.1mm) specimens and by volume elements in the thickness for thick skins (1 mm). In this way, the triaxial stress state of the metallic skin located directly below the indenter was modelled satisfactorily. A fine mesh was created in the contact area just below the indenter to generate a smooth contact law without any slope discontinuity. A sensitivity study of the mesh gave a convergence result if 5 volume elements through the thickness and 36 elements per cell in the contact area were used.

The local rotation θ_i corresponded to the rotation of the upper node of the spring which also belonged to the skin. This local rotation θ_i was obtained directly with Mindlin plate elements but it had to be computed in the case of volume elements for the thick skin (more details can be found in [28]). In both cases, the rotation was assumed to be:

$$\theta_i = \sqrt{R_x^2 + R_y^2} \qquad \text{(eq 2)}$$

where R_x and R_y are the local rotations of the interface nodes between the skin and the spring. The elastic-plastic behaviour laws for brass skins were obtained from conventional tensile tests. Taking advantage of the symmetry of the structure, only one quarter of the plate was modelled. The numerical simulation was limited to 2 mm of indentation, which largely exceeds the threshold value of detectability known as BVID (Barely Visible Impact Damage).

The results of computation were compared to the tests on sandwiches with thin skins (Figure n°12) and a good test/computation comparison was obtained for all three indenter radii. Globally, the undulations observed during the test were also found numerically and cor-

responded to the drop in the load after the peak load of each vertical edges located at the circumference of the indented area. For the thin skin, the rotation always proved to be less than 2.3°. It should therefore be possible to use the simple law with peak F_{wp} for all vertical edges. This is hardly surprising since the skin shapes itself perfectly around the indenter and the test was similar to the one performed with the indenter directly in contact with the honeycomb. However, as lateral folding of the edges could occur with the skin in place, the correlation was good whatever the diameter of the indenter. For the thick skins, if the F_{wp} law was not corrected to take into account the rotation, there was a difference of about 15% between the computational and the experimental results. This can be explained by the fact that the rigid skin did not follow the shape of the indenter when it bent. The bend caused rotations at the menisci before the edges involved had reached peak load [28]. When the rotation is taken into account, the comparison for sandwich structures using thick skin gives a globally acceptable result considering the test dispersion (Figure n°13). For the thick skin, the bending stiffness was 1000 times that of the thin skin and the deformed shape of the skins generated local rotation in the upper edges of the honeycomb. Finally, the finite element model proposed was able to compute the static contact law with acceptable accuracy.

4. Indentation of a structure.

In practice, impacted aeronautical sandwich structures are mostly simply supported or clamped but are never fully supported. From a practical point of view, it is important to know whether or not a coupling effect exists, between the indentation and the stress field generated by the loading. To study this phenomenon, three-point bending tests were undertaken on sandwich plate.

Three Nomex™ honeycomb specimen measuring 220 x 100 mm with 1 mm thick brass skins were produced (Table n°1). Globally, the experimental procedure and manufacturing of the specimen were the same as described previously (see Figure n°15). The distance between the cylindrical steel supports was 200 mm and three displacement sensors (DC3 to DC5) were located on the lower skin to measure the deflection of the specimen. Two displacement sensors (DC1 and DC2) were also located on the upper face of the indenter. Three tests were completed with indenter radii of 21.75 mm, 30.125 mm and 57.25 mm. The depth of indentation was obtained by calculating difference in displacement between the points on the upper and lower skins just below the indenter ((DC1 + DC2)/2 – DC4) in Figure n°15). The force/indentation curves could then be directly compared with those obtained previously from the tests on rigid flat supports (Figure n°16 et Figure n°17) and it was seen that the force/indentation contact laws were superimposed. Experimentally, for the configuration tested, it appears that there is no nonlinear coupling and, consequently, there is a superimposition of global bending and local indentation effects.

When a honeycomb sandwich structure undergoes bending, the transverse shear of the core plays an important part in the deflection and has to be taken into consideration. It is obvious that the proposed modelling of the core by a series of nonlinear vertical springs cannot take this transverse shear stress into account. However, the bending and indentation effects seem to be uncoupled. So, to represent the bending effect of the sandwich, equivalent nodal compression loads were added laterally at the nodes located at the edge of honeycomb block and at the indented skin side (Figure n°18). The computation result of this model was compared to the numerical simulations discussed in paragraph 3.4 and, as shown in Figure n°18, the results were equivalent. This approach enables the practical problem of sandwich structure indentation to be represented, since the bending/indentation uncoupling is again

present. Physically, this uncoupling can be attributed to the existence of a plasticized area at a very early stage, under the indenter area. This area becomes saturated in stress and insensitive to the loading increments on the sandwich skin. The only possible coupling must appear at the initiation of the indentation area, which must logically be earlier when the skin is loaded under lateral compression. However, this phenomenon was not observable for the configuration tested.

At this stage of the study, it is now possible to model the static indentation of metal-skinned sandwich structures. In the finite element model, a grid of nonlinear springs represents the honeycomb. The effects of local rotations of the skin during indentation on the crushing behaviour of the honeycomb are included. The compression law is obtained by a basic compression test on a block of honeycomb.

5-Dynamic study

In the previous paragraph, the possibility of obtaining the static contact law numerically was demonstrated. Nevertheless, in industrial cases the geometry can be more complex with various shapes and different local stiffnesses. So, the objective of this part of the study is to determine whether the approach developed in the last paragraph is suitable to model the dynamic behaviour of sandwich structures with metallic skins under low-velocity and low energy impact.

For this purpose, dynamic impact tests were performed using mass drop test equipment (see Figure n°19). The sandwich plates used for the experiments were of the same type as the ones for the three point bending tests (100x220 mm², core thickness 15 mm, and skin thickness 1 mm). The boundary conditions were also the same (see Figure n°15). The impactor having spherical tip with radii of 30.125 or 57.25 mm, hit the centre of the plate.

The mass of the impactor were respectively 885 et 865 g. The impact speeds recorded were respectively 2,58 and 2,80 m/s. The impact energy was about 3 Joules. The impactor was equipped with a load cell and an accelerator to provide the deflection and the force during the impact. The redundancy of these two data was voluntary. Nevertheless, practically, the force signal gave less interference and it was the only information that was used to measure the force. The force/time and force/displacement curves are shown Figure n°21 and Figure n°22. The complex law of the dynamic contact force should a priori be the superimposition of the dynamic response of the sandwich structure and the local indentation.

To model the dynamic test, two assumptions were made:

- *The global behaviour of the structure did not depend on local response during impact. This hypothesis agrees with the local nature of the impact reported in the literature.*
- *The static/dynamic equivalence was assumed for the range of structures and impacts studied. Thus, it was possible to use the static contact law computed previously.*

With these assumptions, a multi-scale approach could be proposed: the local indentation law was computed first. The only parameter necessary was the crushing law for the spring, which was obtained simply by a basic compression test on a block of honeycomb. As the local dynamic effects were neglected, a nonlinear spring was used to represent the contact law in the global model as shown . The compression law for this spring was the indentation law previously computed in paragraph 3. This proposition is similar to the approach of Choi [32] for laminated plates. An implicit finite element model was made using the same software as in paragraph 3.2. The sandwich structure was modelled by Mindlin plate finite elements (Figure n°20). The materials of the structure were assumed to be linearly elastic. The mass density of

the brass skin and the Nomex were respectively 8000 kg/m³ and 48 kg/m³. The transverse moduli of the core were G_{yz}=44 MPa, G_{xz}=30 MPa and E_{zz}=120 MPa.

Following the assumptions and to avoid local dynamic effects, it was decided to increase the transverse shear modulus of the core artificially on the right of the indenter with the following values: G_{yz}= G_{xz}=5000 MPa. Numerical tests were performed to demonstrate the little influence of the area dimension and the modulus of the local reinforcement on the global response of the structure. In our case, the nonlinear spring law was obtained numerically. The linear stiffness of the spring was 2.67 kN/mm, the yield stress corresponded to a force of 0.4 kN and the plastic stiffnesses were 0.714 and 0.93 kN/mm for the 30.125 and 57.25 indenters respectively. The initial velocities were those measured (2,58 and 2,80 m/s respectively). For the dynamic computation, a Hilbert Hughes Taylor algorithm with automatic time stepping (implicit predictor-corrector scheme) was selected [33].

In spite of the relative simplicity of the model used, the numerical simulations fit the experimental results correctly (Figure n°21 and Figure n°22). The maximum contact force has been found, which will provide the damage area by a return to the indentation model. The static-dynamic equivalence for this range of structures and impacts, which was mainly observed experimentally, has also been confirmed numerically. Besides, the possibility of making indentations on fully supported specimens has been demonstrated. This result also globally validates the approach and the hypotheses made. The simplicity of the model should be an advantage in dealing with complex structures and multi-impact phenomena.

5-Conclusions

A method has been developed to model low velocity/low energy impacts on metal-skinned sandwich structures, and gives good correlation of contact laws. An analysis of the

crushing from a structural point of view has enabled us to propose an original way of modelling Nomex™ honeycomb core using a grid of nonlinear springs. In practice, the springs in implicit finite elements provide a faster and a more robust computation, especially when the stiffness varies and decreases suddenly as is found to occur in brittle materials such as Nomex™. The local rotation of the upper surface of the honeycomb which interfaces with the skin plays a role in the initiation of vertical edge buckling. This interface effect between skin and honeycomb is then taken into account in the model. Direct application of this modelling enables the contact law to be computed when metal-skinned sandwiches are quasi-statically indented on a flat support. This approach gives highly accurate correlation of indentation tests on a flat support or under 3-point bending.

The proposed multi-level approach consists of three steps. Firstly, a basic compression test must be performed on a block of honeycomb to obtain the initial crushing law. Secondly, using this law in nonlinear springs, it is possible to obtain the contact law by a finite element model and a nonlinear static computation. Finally, with the hypothesis of neglecting the dynamic effect at the contact, a basic finite element spring mass model using a nonlinear contact law computed at the last step is able to model a dynamic test. As a good correlation is obtained, the hypothesis of equivalence between static indentation and dynamic test is validated. This basic approach could be useful to model complex structures under impact or multi- impact. It is important to note again that the impact simulation is complete and is, finally based only on a simple economical compression test on a block of honeycomb core. It avoids the use of indentation tests on the complete structure to identify the Meyer's law coefficient. It also shows that the phenomenon remains local and, for the range of structures studied, is independent of the boundary conditions and the dimension of the plate. It would

seem that the approach that has been developed can be used for other cellular cores made from other materials thanks to the similar and common crushing mechanism.

The use of metallic skin in this study enables a step by step approach to the modelling of the impact but this remains a limitation in practice since it is rare nowadays for sandwich structures to be made using metallic skin in industry. The real challenge will still be to couple this modelling approach with laminated skin. In this case, the plasticity behaviour will be replaced by determination of the damage state in both the honeycomb core and the skin and the possible coupling between the stress state of the global structure and the indentation phenomenon will have to be taken into account. Knowing the local state, it will be then possible to compute the residual strength by a second model.

6-References

[1]. Abrate S. Localized impact on sandwich structure with laminated facings. Appl Mech Rev 1997; 50(2): 69-82.

[2]. Guedra-Degeorges D., Thevenet P., Maison S. Damage tolerance of sandwich structures. Proceedings of the Euromech 360 Colloquium, Saint-Etienne 1997,pp 29-36, A Vautrin, Kluwer Academic Publishers.

[3]. Razi H., Sergeev B., Shkarayev S., Madenci E. Analysis of sandwich panels with multiple-site damage. Engineering Fracture Mechanics 1999; 64(2) 255-268.

[4]. Ferri R., Sankar. Static indentation and low velocity impact tests on sandwich plates. Proceedings of the 1997 ASME International Mechanical Engineering Congress and Exposition, Dallas, TX, USA, Vol 55, pp 485-490

[5]. Williamson J., Lagace P. A. Response mechanism in the impact of graphite/epoxy honeycomb sandwich panels. *Proceedings of the 8th technical conference of the American society for composites, Cleveland, OH, USA, pp 287-97, Technomic Publishing Company1994.*

[6]. Herup E. J., Palazotto A. N. Low-velocity impact damage initiation in graphite/epoxy/nomex honeycomb-sandwich plates. Composite science and technology 1997; 57(12): 1581-1598.

[7]. Swanson R.S., Jongman K. Design of sandwich structures under contact loading. Composite Structures 2003; 59: 403-413.

[8]. Soden P. Indentation of composite sandwich beams. Journal of strain analysis 1996; 31(5): 353-360.

[9]. Olsson R., McManus H. L. Simplified theory for contact indentation of sandwich panels. Proceedings of the AIAA/ASME/ASCE/AHS/ASC 36th Structural dynamic and material conference, New Orleans, LA, 1995, pp 1812-1820. AIAA-95-1374-CP

[10]. Bernard M. L., Lagace P. A. Impact resistance of composite sandwich plates. Journal of Reinforced Plastics and Composites 1989; 8(5): 432-445.

[11]. Tsotsis T. K., Lee S. M. Characterization of localized failure modes in honeycomb sandwich panels using indentation. ASTM STP 1274, 1996, pp 139-165.

[12]. R. K. McFarland Jr. Hexagonal cell structures under post-buckling load. AIAA Journal 1963; 1(6): 1380-85.

[13]. Wierzbicki, T. Crushing analysis of metal honeycomb. International journal of impact engineering 1983; 1: 157-74.

[14]. Wierzbicky T, Alvarez A.D.L, Hoo Fatt. M.S. Impact energy absorption of sandwich plates with crushable core. Proc of the joint ASME Applied Mech and Mat Summer Meeting 1995. 205, 391-411.

[15]. Mohr, D. and Doyoyo, M. Deformation-induced folding systems in thin-walled monolithic hexagonal metallic honeycomb, International Journal of Solids and Structures 2004;41(11-12): 3353-3377.

[16]. Mohr, D., Doyoyo, M. Large plastic deformation of metallic honeycomb: Orthotropic rate-independent constitutive model, International Journal of Solids and Structures 2004; 41(16-17): 4435-4456.

[17]. Mohr, D., Doyoyo, M. Experimental Investigation on the Plasticity of Hexagonal Aluminum Honeycomb Under Multiaxial Loading. Journal of Applied Mechanics 2004; 71(3): 375-385.

[18]. Xue Z., Hutchinson J.W. Constitutive model for quasi-static deformation of metallic sandwich cores. International Journal for Numerical Methods in Engineering 2004; 61: 2205-2238.

[19]. Wang, A.J., McDowell, D.L.Yield surfaces of various periodic metal honeycombs at intermediate relative density, International Journal of Plasticity 2005: 21; 285-320.

[20]. Mohr D., Xue Z., Vaziri A., 2006: Quasi-static punch indentation of a honeycomb sandwich plate: experiments and modelling. Journal of Mechanics of Materials and Structures 2006; 1(3): 581-604

[21]. Aminanda Y., Castanié B., Barrau J.J., Thevenet P., Guedra-Degeorges D. Etude expérimentale et modélisation du comportement en compression des structures nid d'abeille. J. Phys IV France 2002:12; Pr11-219 to Pr11-226.

[22]. Thomson R.S., Mouritz A.. P,. Skin wrinkling of Impact Damaged Sandwich Composite. Journal of Sandwich Structures and Materials 1999; 1: 299-322.

[23]. Besant T., Davies G.a.o., Hitchings D. Finite element modelling of low velocity impact of composite sandwich panels. Composite Part A 2001; (32): 1189-1196.

[24]. Qixuan Zheng, Zhengneng Li, Di Wu. Damage analysis of honeycomb core composite sandwich plate subjected low velocity impact. Journal of Reinforced Plastics and Composites 2000; 19(1): 58-68.

[25]. Minguet P.J. A model for predicting the behaviour of impact-damaged minimum gage sandwich panels under compression. Proceedings of the AIAA/ASME/ASCE/AHS/ASC 32th Structural dynamic and material conference, Baltimore, MD, 1991, pp 1112-1122. AIAA-91-1075-CP.

[26]. Horrigan D.p.w., Aitken R.r., Moltschaniwskyj G. Modelling of crushing due to impact in honeycomb sandwiches. Journal of Sandwich Structures and Materials 2000; 2: 131-151.

.

[27]. Aminanda Y., Castanié B., Barrau J.J., Thevenet P.: Experimental Analysis and Modeling of the Crushing of Honeycomb Core. Applied Composite Materials 2005; 12: 213-227.

[28]. Aminanda Y., Castanié B., Barrau J.J., Thevenet P.: Modélisation de l'indentation des structures sandwichs à peaux métalliques. Mécanique et Industrie 2005; 6: 487-498.

[29]. Aminanda Y., Castanié B., Barrau J.J., Thevenet P.: Experimental and Numerical Study of Compression After Impact of Sandwich Structure with Metallic Skins. Composite Science and Technology, Special Issue on JNC 14, to be published.

[30]. Michael Chun Yung Niu. Airframe structural design. Hong Kong: Conmilit Press; 1997.

[31]. Jean-jacques Barrau, Serge Creze And Bruno Castanie: Buckling and post-buckling of beams with flat webs. Thin-Walled Structures 2005; 43(6): 877-1002.

[32]. Choi I.K, Lim C. H.: Low-velocity impact analysis of composite laminates using linearized contact law. Composite Structures 2004; 66: 125–132

[33]. Samcef Users Guide. SAMTECH, Liège, Belgium

Tables.

.

SANDWICH MATERIALS	Skin thickness	Specimen size	Number
Skin : Brass	0.1 mm	100*100 mm	6
Core : Nomex (HRH 78,1/8,3)	1 mm	100*100 mm	6
48 kg/m3, 15 mm thick	1 mm	220*100 mm	6

Table N° 1: Detail of the sandwich specimens built.

FIGURES.

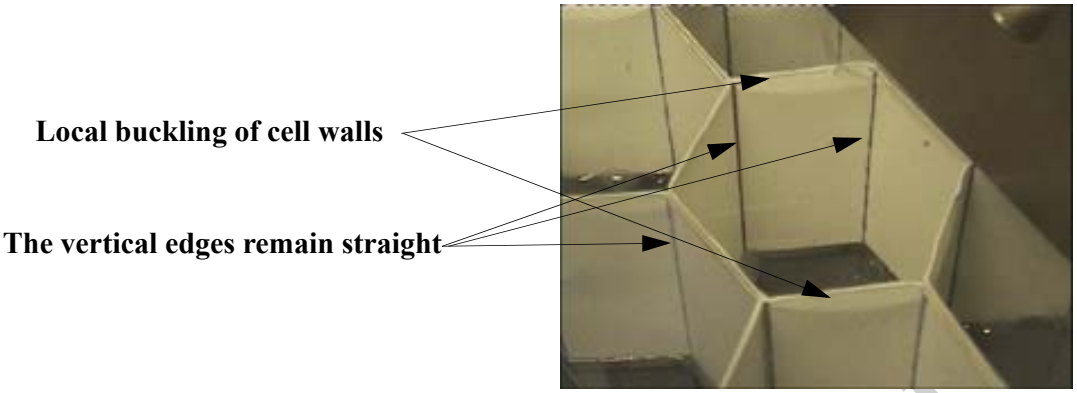

Figure N° 1: Mechanism of crushing for a one-skin paper specimen.

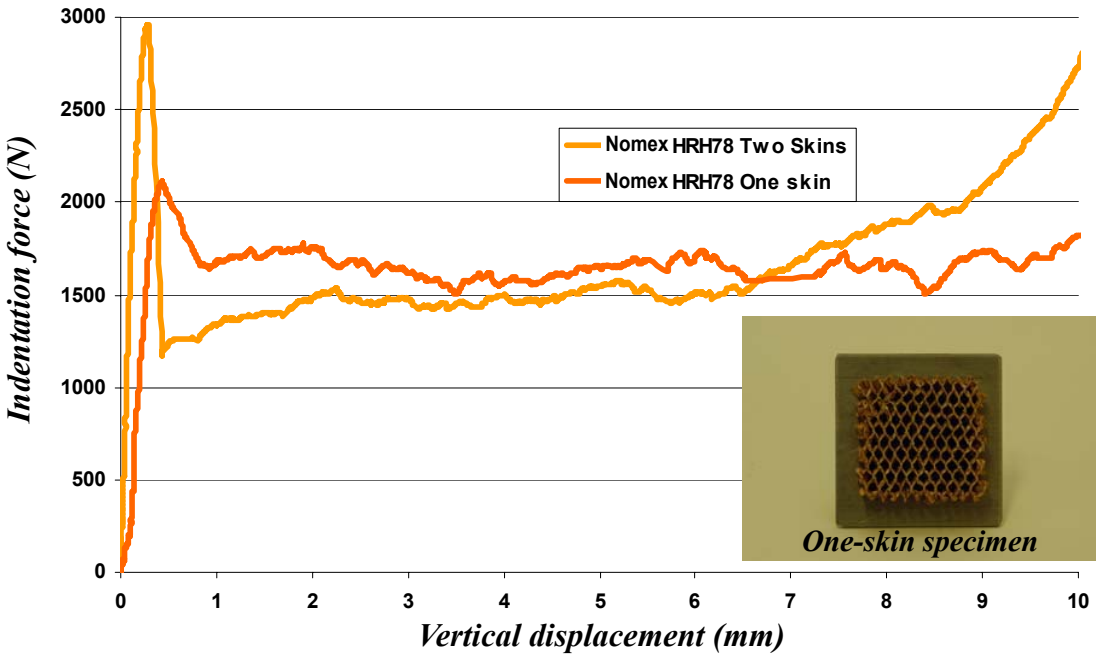

Figure N° 2: Compression test curve of the block.

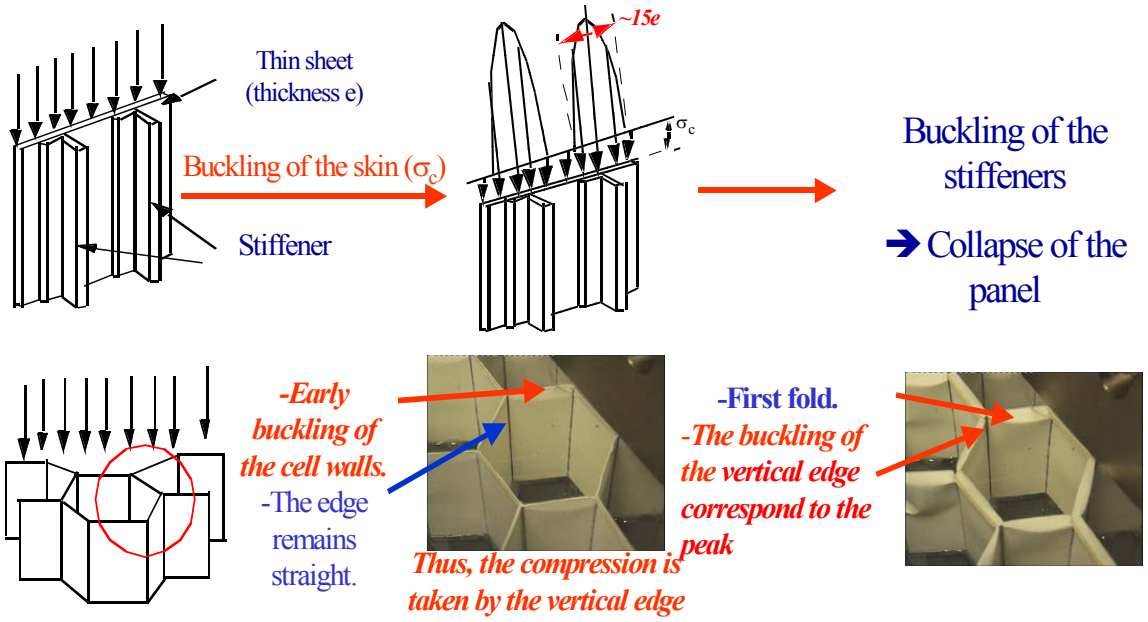

Figure N° 3: Analogy with the buckling of stiffened panels.

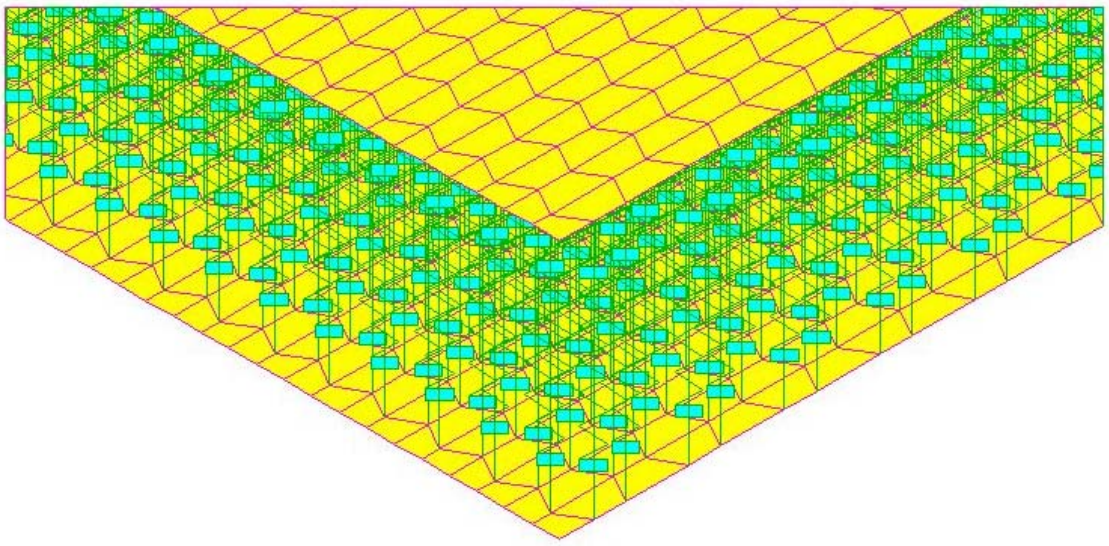

Figure N° 4: Sample of discrete modelling of honeycomb core.

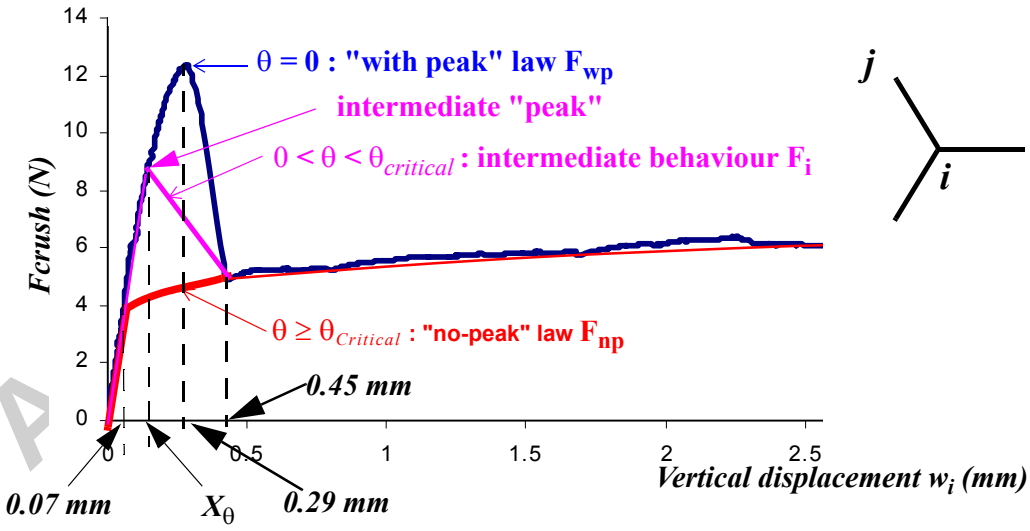

Figure N° 5: Generalized crushing law $F_{Crush}(w_i, \theta_i)$ of cell edge i.

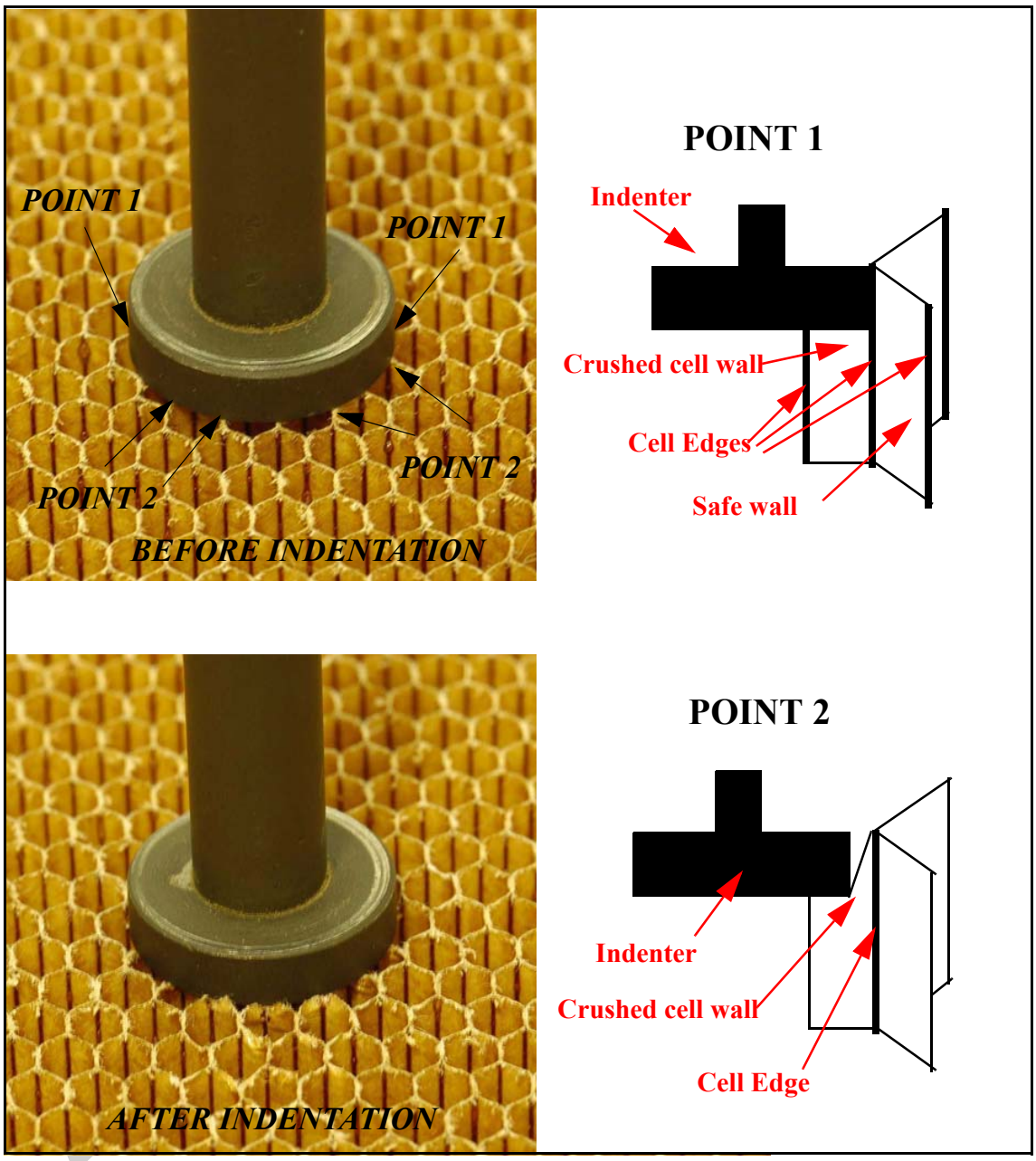

Figure N° 6: Description of the indentation test with a cylindrical indentor.

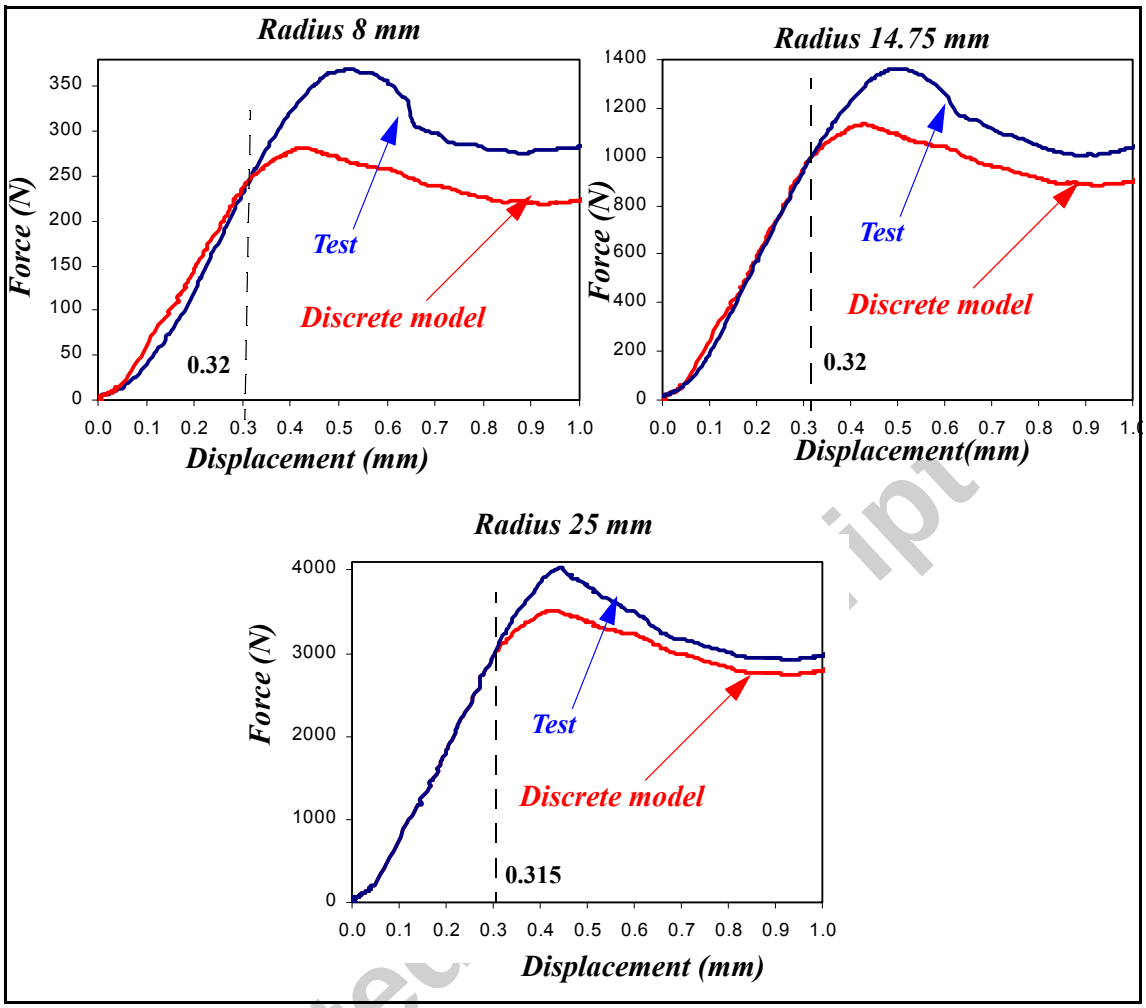

Figure N° 7: Experimental contact law with cylindrical indenter and discrete model comparison.

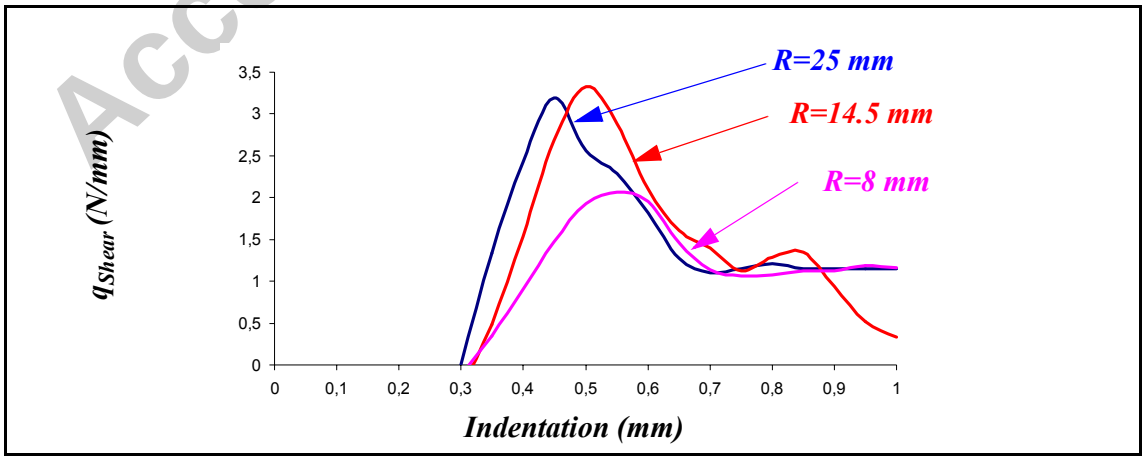

Figure N° 8: Peripheral shear force per unit length.

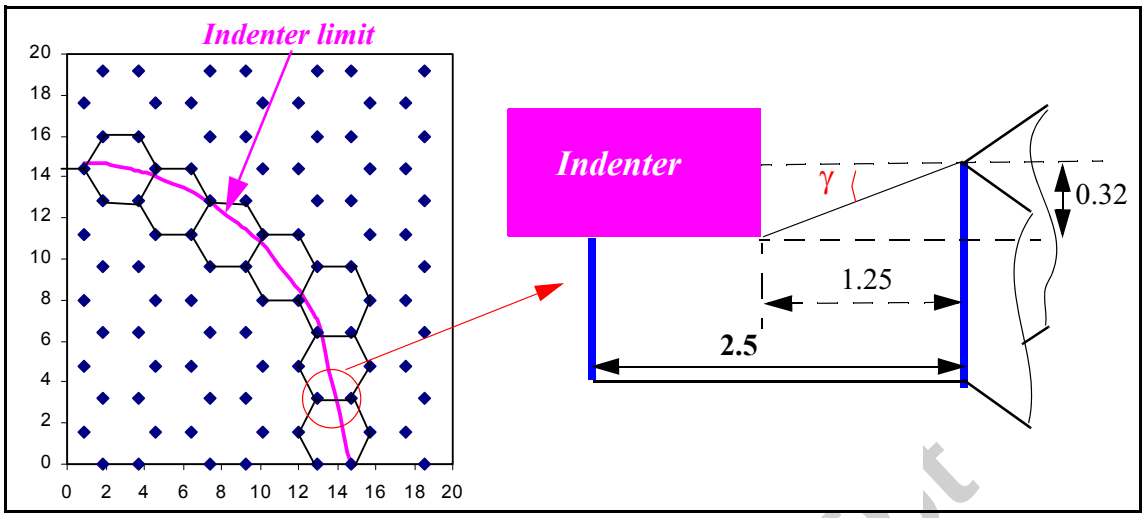

Figure N° 9: Geometry for the computation of the limit γ.

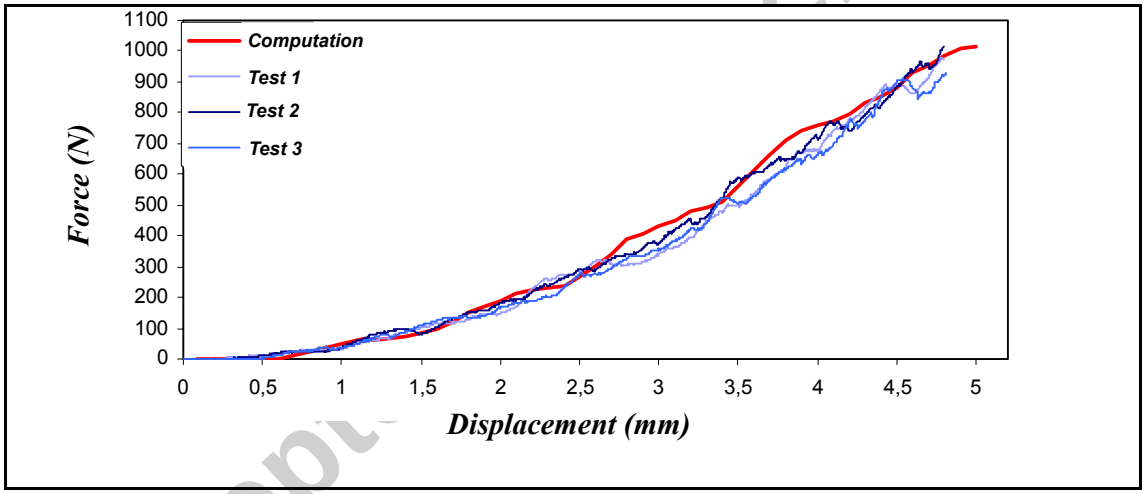

Figure N° 10: Comparison between calculation and indentation tests with conical indenter (Angle: 18°).

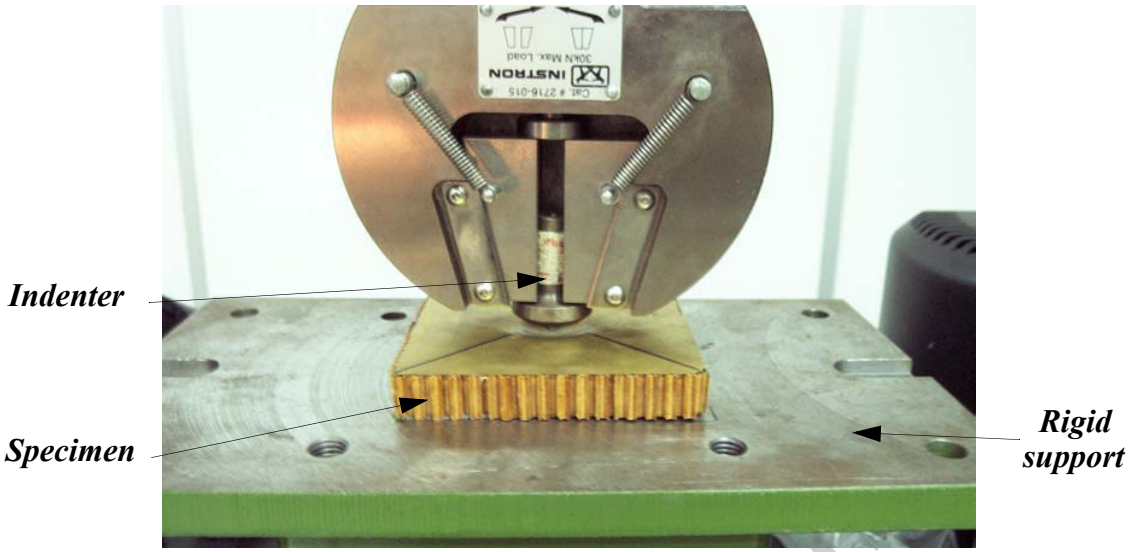

Figure N° 11: Description of the indentation tests on sandwich specimens.

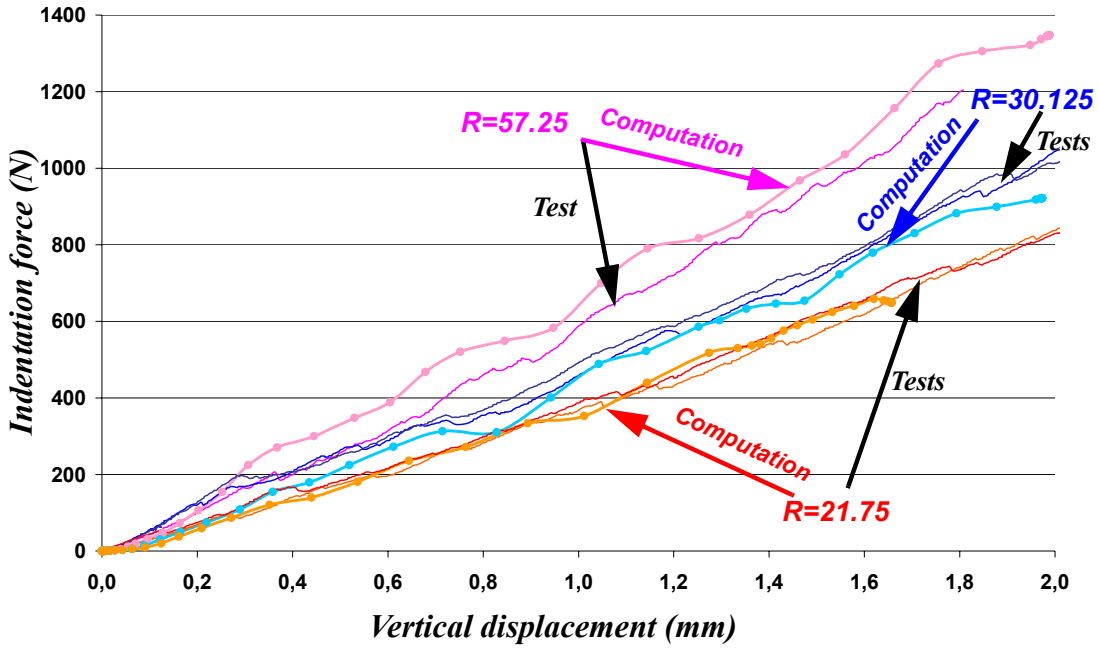

Figure N° 12: Test/numerical model correlation in the case of sandwich with thin metal skins.

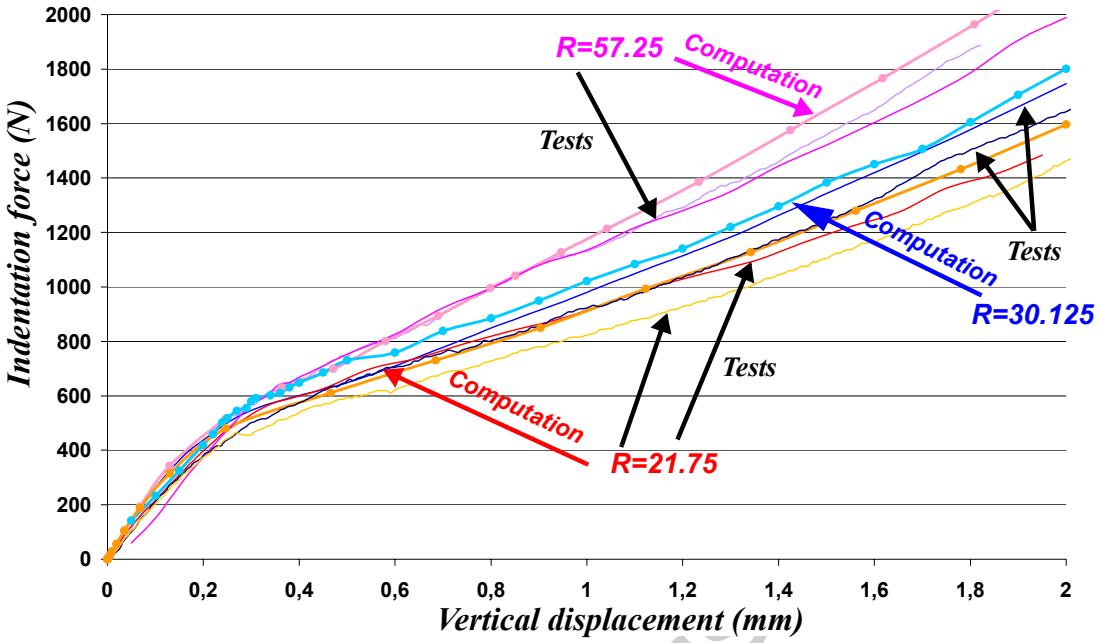

Figure N° 13: Test/numerical model correlation in the case of sandwich with thick metal skins.

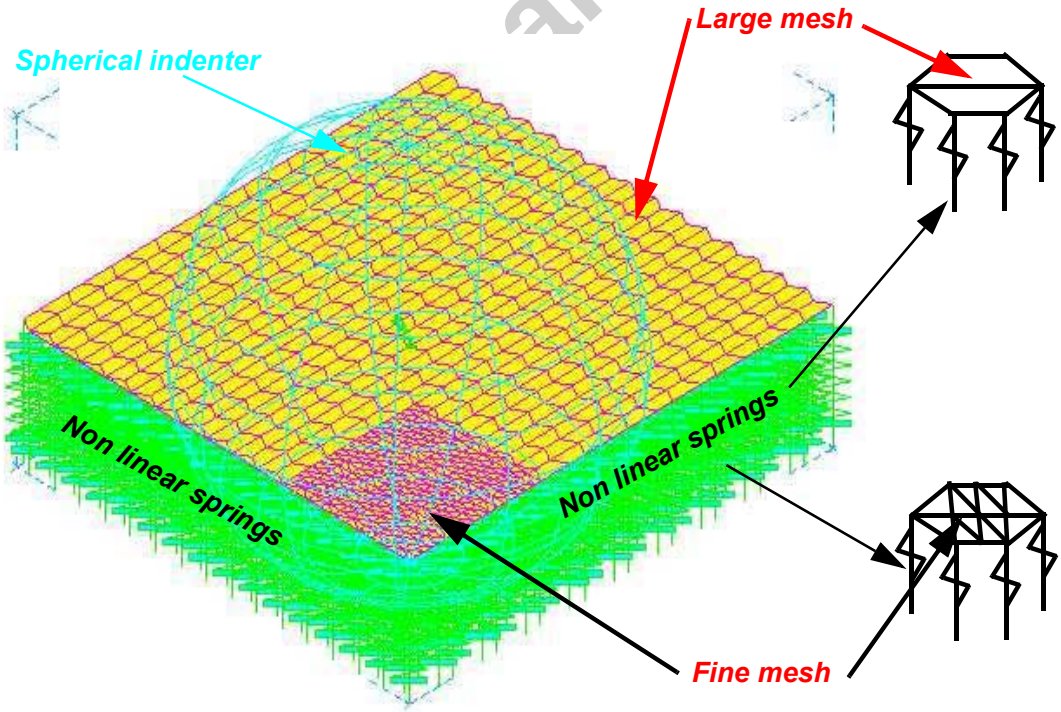

Figure N° 14: Finite element modelling of the indentation problem on sandwich with thin metal skins.

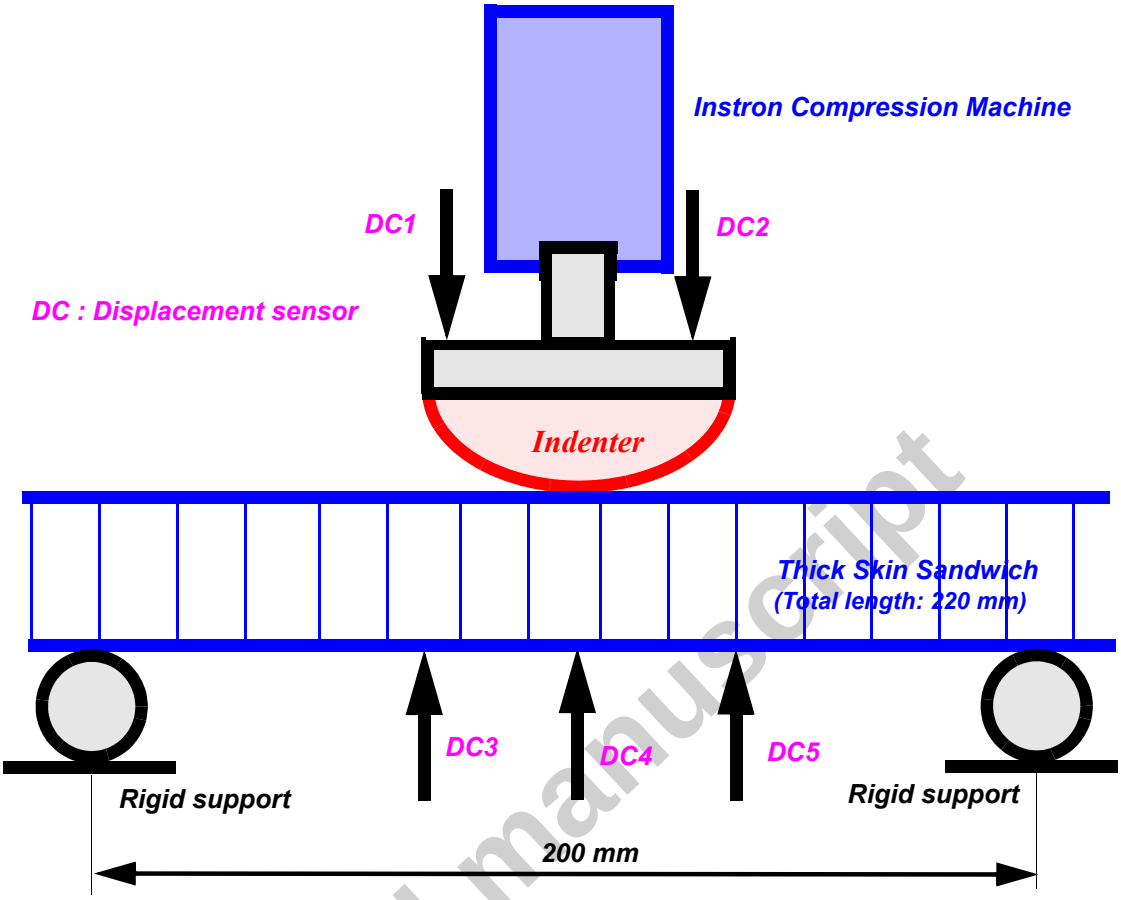

Figure N° 15: Three-point bending test principle.

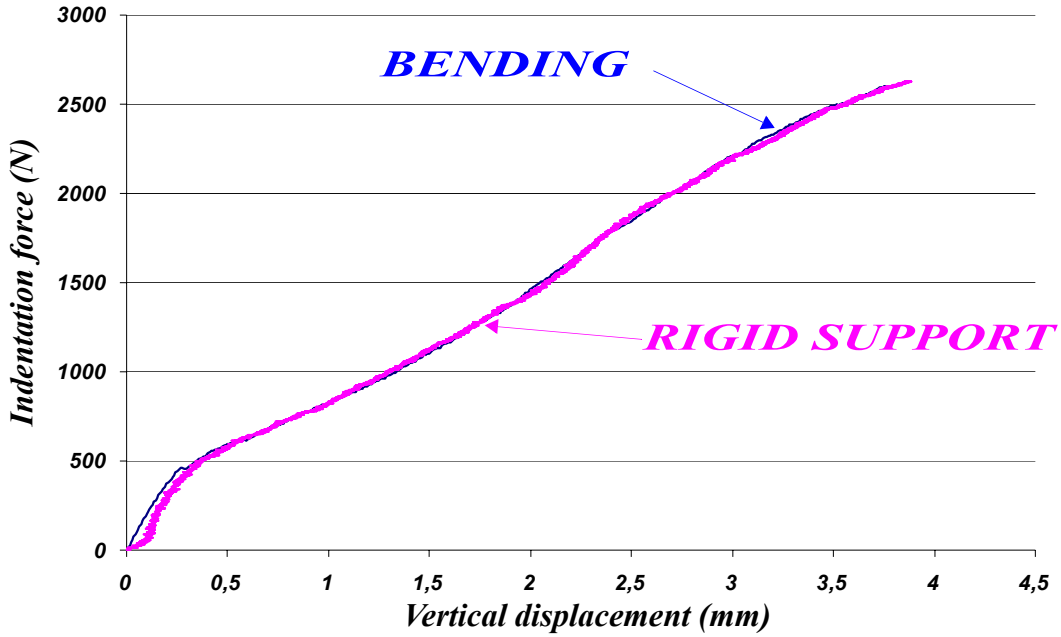

Figure N° 16 : Comparison of the force/crush experimental curves in the case of rigid support and 3-points bending, indenter R = 21.75 mm.

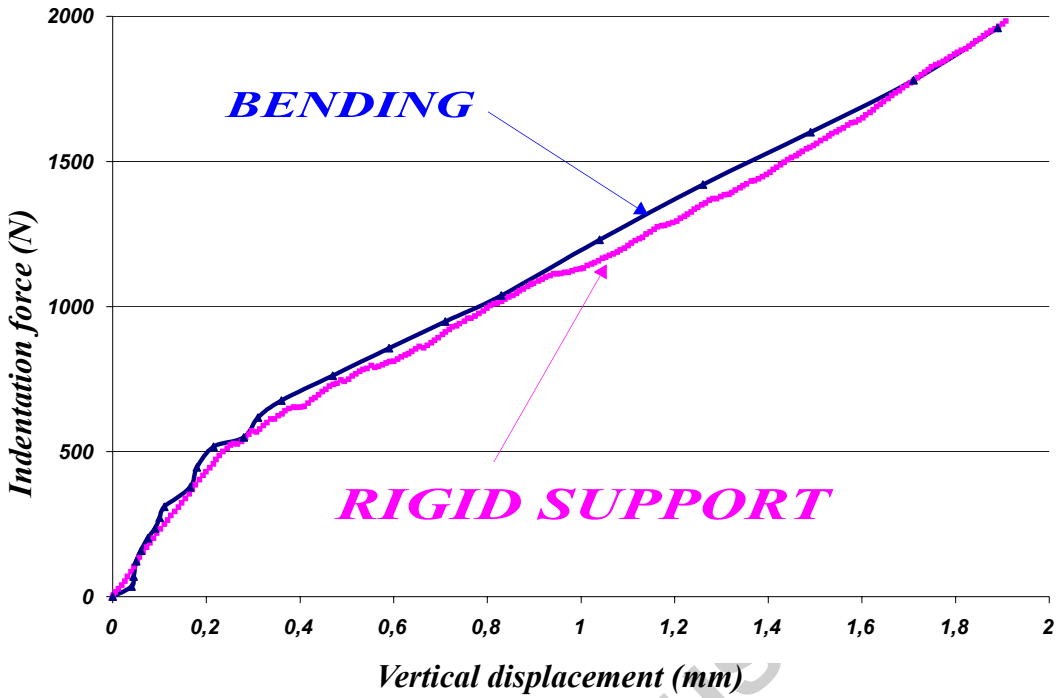

Figure N° 17: Comparison of the force/crush experimental curves in the case of rigid support and 3-points bending, indenter R = 57.25 mm.

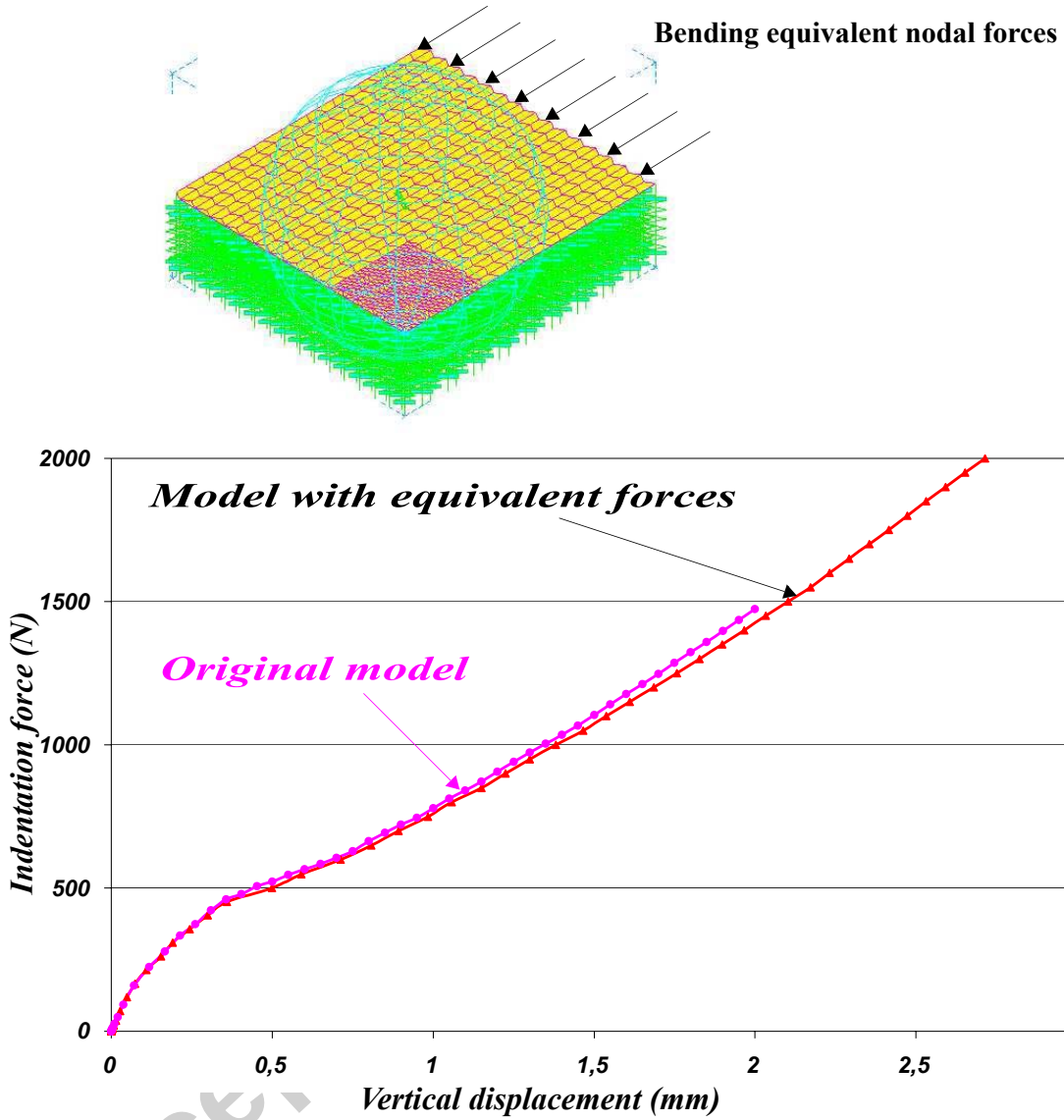

Figure N° 18: Adapted model in indentation for bending loads and comparisons between previous modelling and the model with nodal forces, for indenter 21.75 mm.

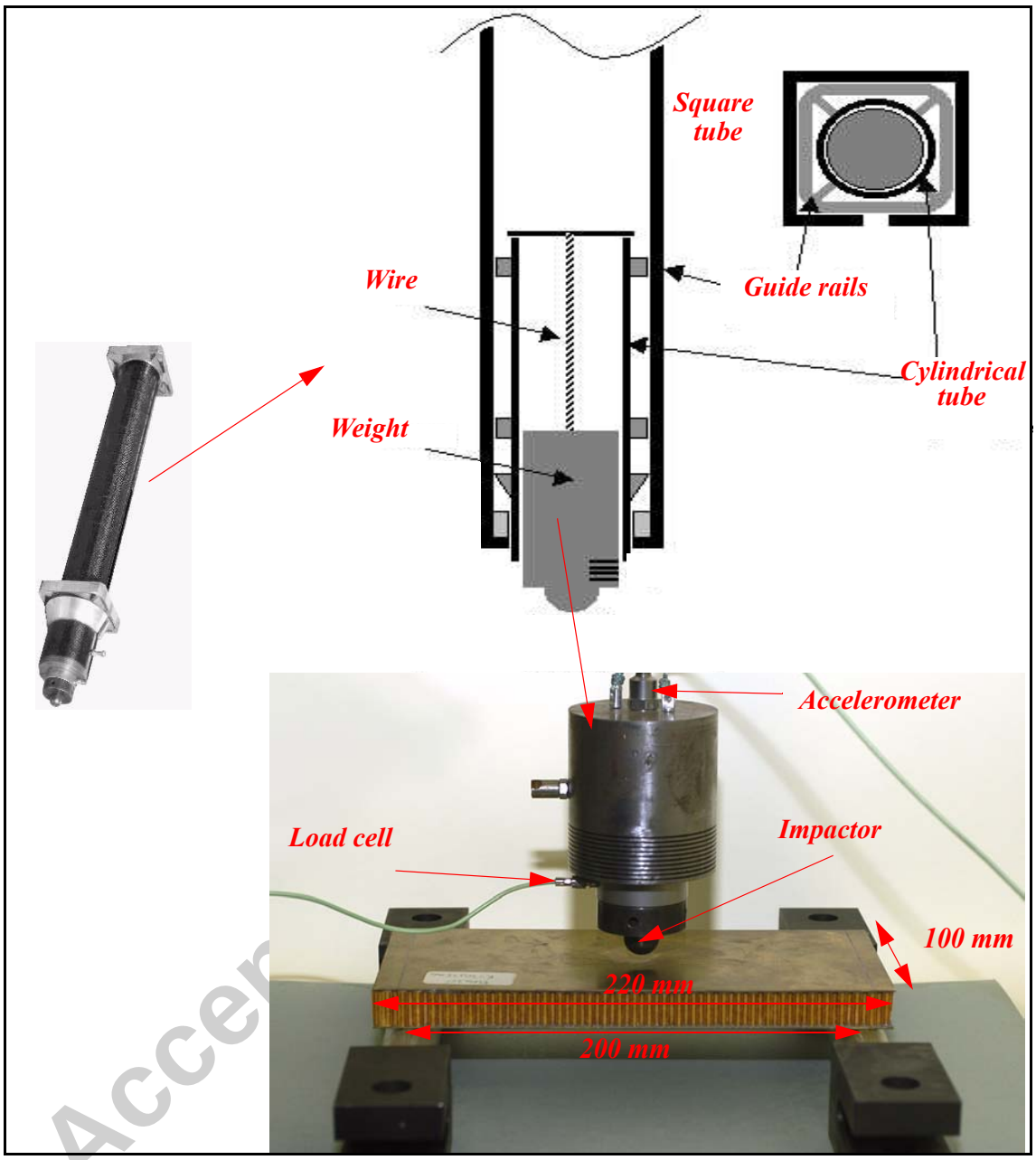

Figure N° 19 : Load drop test rig.

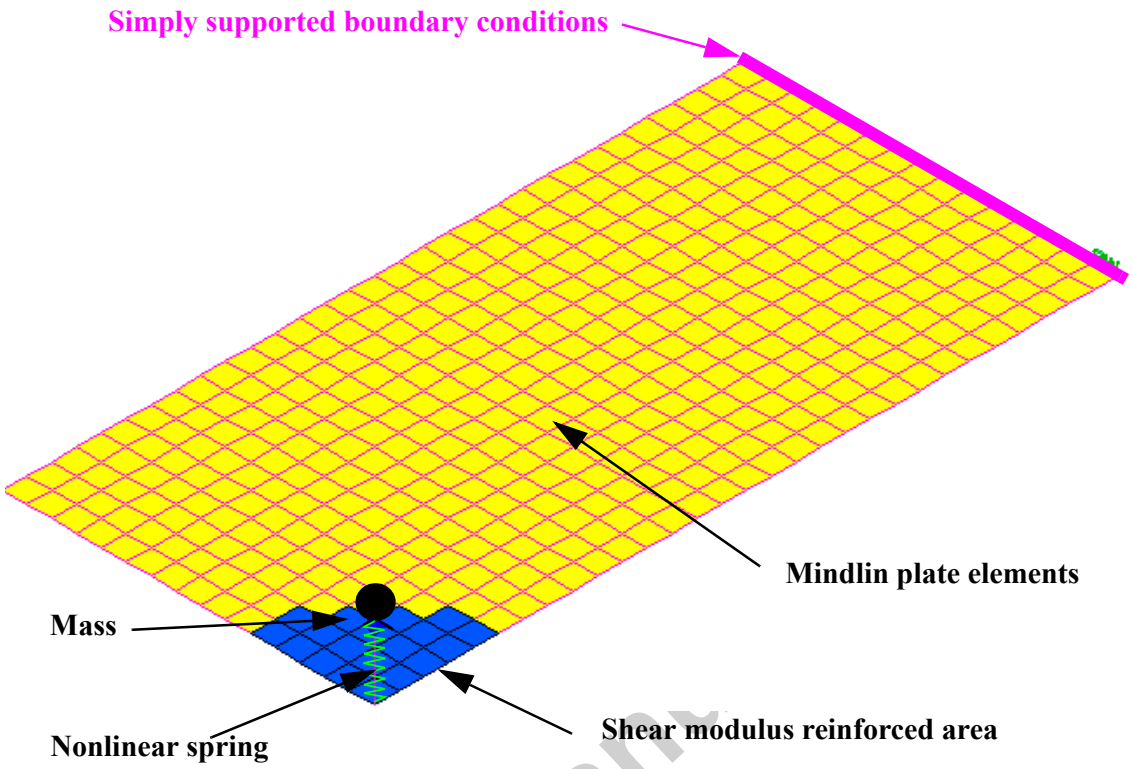

Figure N° 20: Spring-mass finite element model.

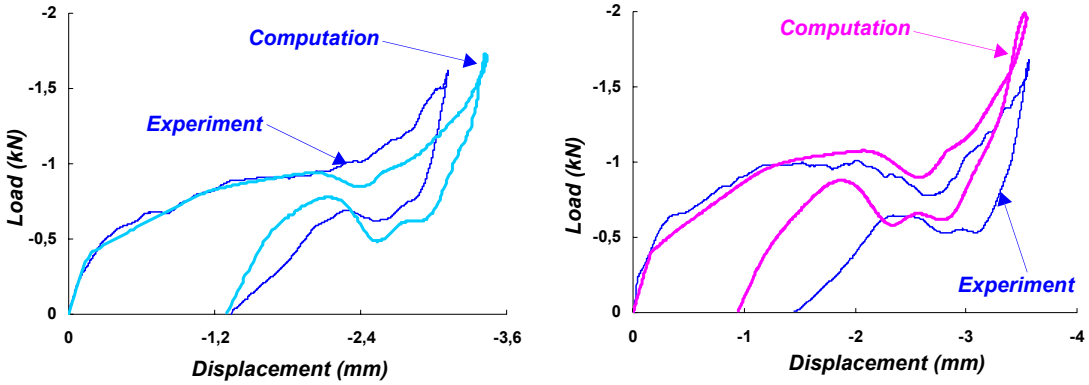

(a) Impactor 30.125 mm *(b) impactor 57.25 mm*

Figure N° 21: Dynamic load-displacement law (a) impactor 30.125 mm, (b) impactor 57.25 mm.

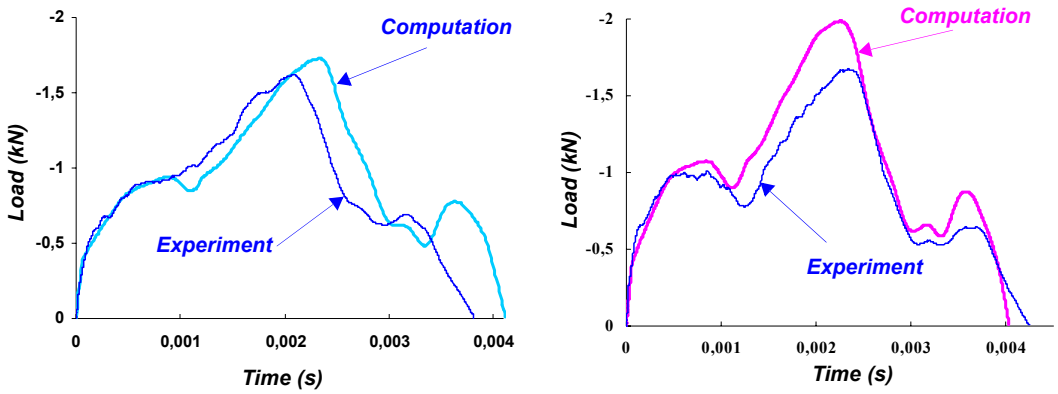

(a) Impactor 30.125 mm (b) impactor 57.25 mm

Figure N° 22 : Dynamic load-time law (a) impactor 30.125 mm, (b) impactor 57.25 mm .